

Toward creating wide-band uniaxial left-handed materials with small losses

C. R. Simovski

Department of Physics, State Institute of Fine Mechanics and Optics
Sablinskaya Street, 14, 197101, St. Petersburg, Russia
Fax: 7-812-2322307; email: simovsky@phd.ifmo.ru

Abstract

In this work a possible realizations of a uniaxial variant of left-handed material (LHM) at microwaves is considered. The meta-material has some features of the known structure studied by the group of D. Smith in 2001, however in the present structure a lattice of parallel wires and a lattice of artificial magnetic resonators (MRs) are unified and the MRs are not split-ring resonators. The optimizing of MRs allows significantly decrease the magnetic losses and broaden the band within which the meta-material becomes a LHM.

1. Introduction

Since 2000 the left-handed media (LHM) first introduced in [1] has become a subject of an abundant discussion mainly due to J. Pendry [2]. In 2001, the negative refraction in a prism of LHM was demonstrated at microwaves [3]. This result has been reproduced in [4] and [5] and now is considered by the scientific community as a reliable one. Negative real part of effective permittivity ϵ_{eff} in the two-phase composite studied by D. Smith, R. Shelby and S. Schultz in their work [3] was created by an array of parallel conducting wires (the wire axis x is the optical axis of this composite medium). The negative value of the real part of permeability μ_{eff} was provided by artificial magnetic resonators (MRs) performed as double split-ring resonators (SRRs). The known SRRs are two coplanar [6] or parallel [7] split wire rings. The negative permeability arises due to the resonance of the magnetic polarizability of SRRs within a narrow sub-band which belongs to their resonant band. This sub-band lies in the wide frequency range where $\text{Re}(\epsilon_{eff}) < 0$ (more exactly this is the real part of the xx -component of the permittivity tensor). As a result, the material becomes a uniaxially anisotropic LHM within this sub-band. Electromagnetic waves in this LHM suffer the magnetic and electric losses. There has been many papers written about these losses since the work [8] in which the structure tested in [3] was treated as very lossy and claimed therefore not to be a LHM. Comparing the results obtained in [8]–[10] with the results of [11] we can see that different simulations of the same structure (Smith-Shelby lattice) give very different results for its losses. Experimental data do not fit with all these simulations and give moderate values for transmission losses per unit thickness in the LHM regime (see [5] and [4]). In the paper [12] the influence of the electromagnetic interaction of SRRs with wires to the losses in this medium has been explained. One has obtained for $\text{Im}(\mu_{eff})$ the values of the order $0.1\text{Re}(\mu_{eff})$ within the band where $\text{Re}(\mu_{eff}) < 0$, $\text{Re}(\epsilon_{eff}) < 0$. It is clear, that the losses are rather significant in this structure. These losses can be slightly reduced increasing the thickness of wires from which SRRs are fabricated, but this increase is restricted by the need to have the strong magnetic resonance. Another short of this structure is a narrow frequency band in which the meta-material is a LHM (in [3] this band was equal few tens of MHz centered at 4.5 GHz).

In the literature one can find alternative versions of a LHM at microwaves, e.g. [13] and [14]. In [13] the self-consistent analytical theory of the quasi-isotropic lattice of metal bianisotropic (Omega) particles has been presented, and the negative parameters predicted within the rather large band 8.2...8.4 GHz. However, the losses were neglected in this work. In [14] the experimental testing of a LHM made from SRRs combined with capacitively loaded strips (instead of long wires) has been done. The aim of [14] was to match this medium with free space. The measured losses turned out to be very high ¹, and the band in which both material parameters extracted from measured data have negative real parts is rather narrow. In Fig. 14 (b) it can be detected as 50 MHz (centered at 9.5 GHz²). In [15] the transmittance through the layer of a racemic medium from resonant chiral particles was calculated. This medium also exhibits negative real part of constitutive parameters within the resonant band of particles. The result for the resonant losses was also pessimistic [15].

In the present paper we suggest another uniaxial variant of LHM structure. The structure is drawn in Fig. 1, on top. The model developed below describes an infinite square lattice prepared from wires located in a homogeneous dielectric host medium of permittivity ϵ_m . Note, that the properties of the similar structure prepared with the use of planar technology and shown on bottom of Fig. 1 are expected to be similar. This must be so if the lattice period D is small enough compared with the wavelength. Then the dielectric board is practically a mixture and its averaged response to the field must be close to that of the host medium with certain effective permittivity ϵ_m (lying between that of free space and that of the dielectric plates). Though a metal strip of width w possess more significant ohmic losses per unit length than a wire with round cross section of same diameter w , the frequency dependence of these losses is approximately the same in both cases. Therefore one can practically find an equivalent radius of the round wire r_0 for given w . Replacing the host medium by the board of dielectric plates and the round wires by the strip wires we theoretically do not change the low-frequency properties of the structure. This makes the variant of LHM with loaded loops shown in Fig. 1 realizable in scientific laboratories. The procedure of obtaining such lattices (using vertical slits) is rather simple. It has been described in [18] and recently used by Dr. Sauviac from the laboratory DIOM (University of St. Etienne, France) for preparing the prototype of the left-handed composite introduced in [13] (its preliminary experimental study is presented in [19]). The main difference between structures drawn on top and on bottom of Fig. 1 is that the structure on top contains one straight wire in a unit cell and the structure on bottom contains two wires. This difference is not crucial.

The MRs suggested in the present paper are long loops (their length $2l$ is of the order $\lambda/2$). It is also assumed that $2l$ is rather close to D_x (the period of loops along the x -axis). Each loop contains two symmetrically located equivalent lumped loads. The width of the loop $2d$ is small ($2d \ll D \ll \lambda$). In Fig. 1 we have shown the case of an inductive load $Z_0 = j\omega L_0$ performed as a small planar spiral (a conventional lumped inductance at microwaves). Linear chains of MRs are electrically connected with the short wires. These line chains operate as straight thick wires being excited by the electric field and as linear arrays of MRs being excited by the magnetic field. Unifying the wires and MRs as it is shown in the Figure allows increase the effective radius of wires and reduce the ohmic losses. The suggested geometry of a MR helps to obtain a rather wide band for an effective LHM (below an example with 120 MHz at 7 GHz is given) in which the $|\text{Im}\mu_{eff}| \ll 0.1|\text{Re}\mu_{eff}|$. Imaginary part of ϵ_{eff} is always smaller than $|\text{Im}\mu_{eff}|$.

¹The mini-pass-band which theoretically corresponding to negative material parameters is almost invisible within the band of the resonant absorption of SRRs, judging on the plots of the transmittance for a 290 mil-thick (7.25 mm) layer. This plot is shown in Figs. 10 and 14a.

²In Fig. 17 there is another band of negative $\epsilon_{eff}, \mu_{eff}$ (10.9 – 11.1 GHz), however at these frequencies the lattice period becomes larger than $\lambda/4$ and the usual constitutive parameters are not physically sound.

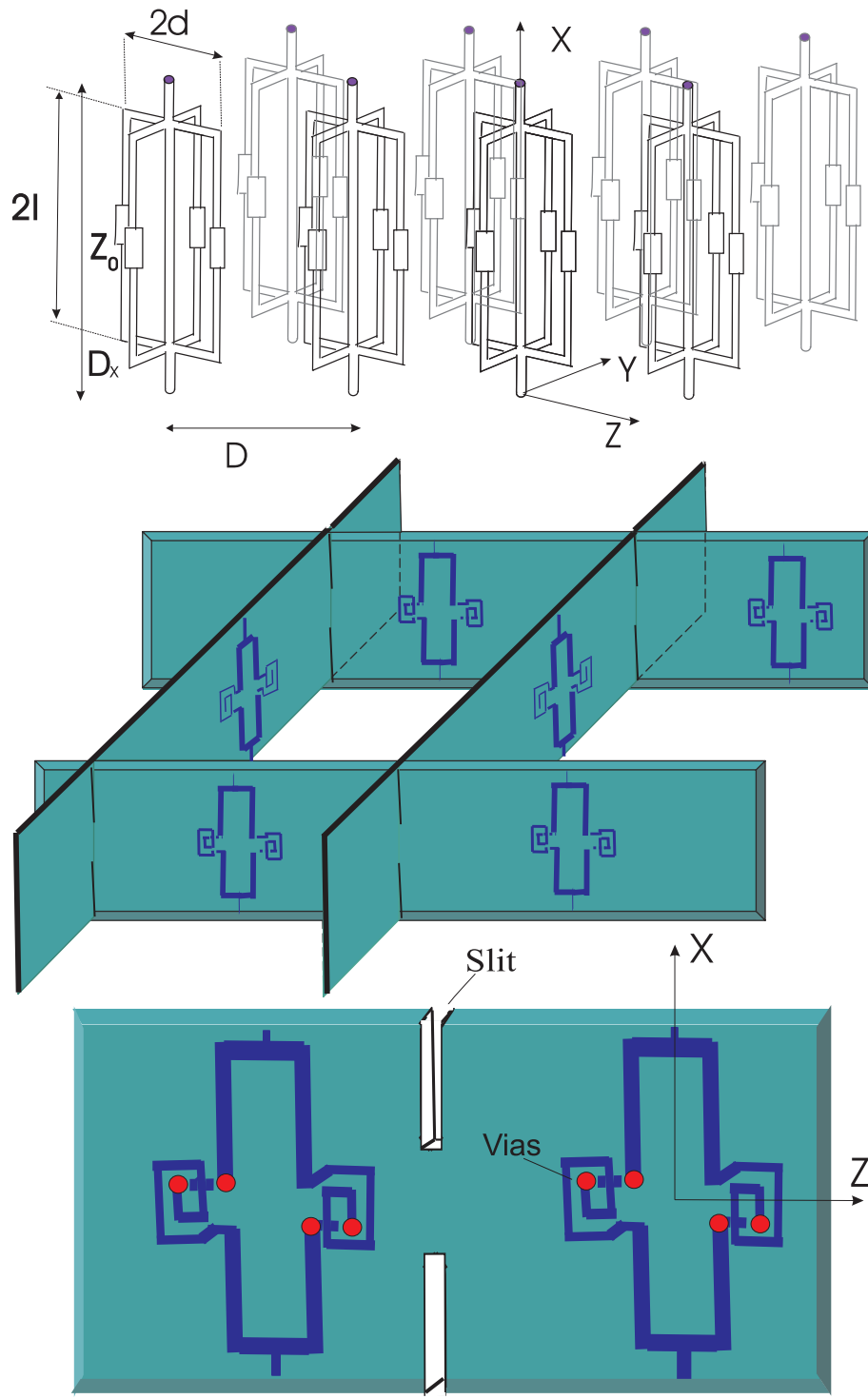


Figure 1: Structure under study (on top) and the idea of its planar realization (on bottom). Inductive loads are performed as planar spirals with conducting vias.

2. Dispersion equation

Let us consider a square lattice with step $D_y = D_z = D$ of chains presented in Fig. 1, on top. Let the wave with unknown propagation constant β (that of the main Bloch mode) propagates along z . To obtain a dispersion equation of the lattice one can consider the response of the chain to the \mathbf{E} -field and \mathbf{H} -field averaged over the plane $(x - y)$ and directed along x and y , respectively. Let us denote these averaged values as $\langle E \rangle$ and $\langle H \rangle$, respectively. The scale of averaging along x is D_x , and along y it is D . The electric field $\langle E \rangle$ excites two orthogonal loops stretched along the x -axis (see Fig. 1) as a thick wire because the induced currents will be parallel in all four sides of the two orthogonal loops (at $x = \pm d$, $y = 0$ and $y = \pm d$, $x = 0$). To this equivalent thick wire an effective radius ρ can be attributed, and it is clear that $r_0 < \rho < d$, where r_0 is the radius of the real wire cross section. So, the chain excited by field $\langle E \rangle$ operates as a wire with radius periodically changing along x from real wire radius to ρ . This periodicity of the radius along x has no impact to the waves propagating orthogonally to x and we can approximately consider our chain excited by electric field as a wire with effective uniform radius r . In our numerical example below we have chosen $r = d/10 = 0.1$ mm, whereas the radius r_0 of the wire forming the loops has been assumed to be equal $r_0 = 0.02$ mm. We do not know the exact relations between r_0 and r , however the ratio $r/r_0 = 5$ can be, of course, realized in practice. This is so, because there is a free parameter for tuning the equivalent radius r : the radius of the wire connecting two adjacent loops. We will see below that the value of r_0 is important for calculating the ohmic losses in the MRs and (as a result) for magnetic losses in the lattice.

We conclude that the electric excitation of the array of parallel chains located in the plane $(x - y)$ (see Fig. 1) is equivalent to the excitation of a mesh of parallel wires with radius r and period $D_y = D$. The grid impedance Z_g of the wire mesh is well-known. It relates the averaged surface current J of the mesh with $\langle E \rangle$ and can be found from the following relations (see e.g. in [20]):

$$\langle E \rangle = Z_g J = \frac{j\eta\alpha}{2} J, \quad \alpha = \frac{kD_y}{\pi} \log \frac{D_y}{2\pi r} .lgrid \quad (1)$$

Here $\eta = \sqrt{\mu_0/\epsilon_0\epsilon_m}$ is the wave impedance of the host medium. This approach allows to consider an array of chains excited by electric field as a sheet of electric current J . Then the lattice in which the chains are excited by electric field can be treated as a set of parallel sheets of electric current.

Relations $\dot{g}rid$ are accurate enough for dense wire grids ($kD < 1$) and are valid for the lossless case. In the present paper we compare the result obtained for our structure with results for the lattice of wires and SRRs obtained analytically in our work [12]. In the cited work we took into account the finite conductivity of straight wires but it practically did not change the result compared to the case of the perfect wires. In accordance with [12] the wave attenuation is practically due to the finite conductivity of SRRs. Therefore in our comparison with [12] we will neglect the lossy part of Z_g but we will take into account the ohmic losses in MRs.

Now let the same array of chains in the $(x - y)$ plane be excited by field $\langle H \rangle$. First, notice that the loops of the reference chain (see Fig. 1) lying in this plane are not excited by y -directed magnetic field. The chain is excited due to the loops lying in the $(x - z)$ plane. Using Maxwell's equation

$$-j\omega\mu_0 \langle H \rangle = \frac{d\langle E \rangle}{dz} \approx \frac{1}{2d} (\langle E \rangle (z = d) - \langle E \rangle (z = -d))$$

we easily obtain that the magnetic excitation of the chain is the same as if the wire located at $z = d$ was excited by x -directed electric field $E = j\omega\mu_0 d \langle H \rangle$, and the wire located at $z = -d/2$ was excited by electric field $E = -j\omega\mu_0 d \langle H \rangle$.

Then we can find the effective voltage \mathcal{E} exciting the loop using the method of induced electromotive forces:

$$\mathcal{E} = \int_L \langle E \rangle (\tau) f(\tau) d\tau,$$

where $f(\tau)$ is the current distribution along the contour L of our loop, normalized to the induced current I_0 taken at the point to which the voltage \mathcal{E} is referred. Let us refer \mathcal{E} to the center of the loop (to a point of the lumped load). Then this voltage is connected to two shortened lines of length l in series with two lumped loads Z_0 . The current distribution in the shortened line of length l is approximately sinusoidal and has the maximum at the shortcut point ($x = \pm l$):

$$I(x) = I_0 f(x) = I_0 \cos k(x - l) / \cos kl.$$

Here $k = \phi \sqrt{\epsilon_0 \epsilon_m \mu_0}$ is the wave number of the host medium. Then we obtain

$$\mathcal{E} = -4j\phi\mu_0 \frac{\tan kl}{k} d \langle H \rangle .lemf \quad (2)$$

If $kl \ll 1$ formula emf transits to the Faraday formula $\mathcal{E} = -j\phi\mu_0 S \langle H \rangle$, where $S = 4dl$ is the area of the loop. The impedance to which the voltage \mathcal{E} is connected is

$$Z = 2(R + jW \tan kl + Z_0) = 2R + 2j(W \tan kl + X_0), lzz \quad (3)$$

where X_0 is the loading reactance, R is the ohmic resistance of the line, W is its wave impedance [16]:

$$R = \sqrt{\frac{\mu_0 \phi}{2\pi^2 \sigma}} \frac{l}{r_0 \sqrt{1 - \left(\frac{2r_0}{d}\right)^2}}, \quad W = \frac{\eta \log \frac{d}{r_0}}{\pi}.$$

In $\dot{z}z$ we neglected the radiation resistance of the loop, however, it does not lead to a mistake because in regular arrays the radiation resistance is suppressed by the interaction of the array elements [17].

We find the current as $I_0 = \mathcal{E}/Z$ and then find the magnetic moment per unit length of a chain defined as $m = 2d\mu_0 \langle I \rangle$, where $\langle I \rangle$ is the averaged (along x) value of the current I :

$$\langle I \rangle = \frac{2I_0}{D_x} \int_0^l f(x) dx.$$

The magnetic moment per unit surface of the plane ($x - y$) is related with m as $M = m/D_y = 2d\mu_0 \langle I \rangle / D$. Then

$$M = \frac{2d\mu_0 \mathcal{E}}{DZ} .lmm \quad (4)$$

Below we use the magnetic susceptibility of the reference sheet (located in the plane ($y - z$)) defined as $a_{mm} = M / \langle H \rangle$. Substituting emf and $\dot{z}z$ into $\dot{m}m$ we obtain for this susceptibility the relation

$$\frac{1}{a_{mm}} = [-(W \tan kl + X_0) + jR] \left(\frac{kl}{\mu_0 S \tan kl} \right)^2 \frac{S_0}{\phi} .lfin \quad (5)$$

Here S_0 is the area of the mesh unit cell $S_0 = D_x D$. If the load is capacitive $X_0 = 1/\phi C_0$ and the loop is electrically small $kl \ll 1$ formula fin gives a well-known result for a split-ring resonator (see [6]):

$$a_{mm} = G \frac{\phi^2}{\frac{1}{L_{\text{loop}} C_0} - \phi^2 + j \frac{R}{L_{\text{loop}}} \phi},$$

where G and L_{loop} are constants and the constant $L_{loop} = Wl\sqrt{\epsilon_0\epsilon_m\mu_0}$ plays role of the effective inductance of the long narrow loop.

Our lattice excited by an electromagnetic wave is a set of parallel magneto-dielectric sheets with electric susceptibility $a_{ee} = 1/Z_g$ and magnetic one a_{mm} . These susceptibilities are defined as

$$J = a_{ee} \langle E \rangle, \quad M = a_{mm} \langle H \rangle. \quad (6)$$

Each sheet produces a plane wave. Let us enumerate the sheets so that the reference one has number $n_z = 0$ (then $M = M(n_z = 0)$ and $J = J(n_z = 0)$). Since $M(n_z)$ and $J(n_z)$ satisfy

$$M(n_z) = M(0)e^{-jn_z\beta D}, \quad J(n_z) = J(0)e^{-jn_z\beta D},$$

we easily obtain for the **E**-field and **H**-field in the reference plane the following set of relations:

$$\langle E \rangle = \langle E \rangle^J + \langle E \rangle^M, \quad \langle H \rangle = \langle H \rangle^J + \langle H \rangle^M,$$

$$\begin{aligned} \langle E \rangle^M &= \frac{j\phi M}{2} \sum_{-\infty}^{\infty} \frac{n_z}{|n_z|} e^{-jn_z\beta D - jk|n_z|D}, \\ \langle H \rangle^J &= \frac{J}{2} \sum_{-\infty}^{\infty} \frac{n_z}{|n_z|} e^{-jn_z\beta D - jk|n_z|D}, \\ \langle E \rangle^J &= -\frac{\eta J}{2} \sum_{-\infty}^{\infty} e^{-jn_z\beta D - jk|n_z|D} \end{aligned}$$

and

$$\langle H \rangle^M = \frac{j\phi M}{2\eta} \sum_{-\infty}^{\infty} e^{-jn_z\beta D - jk|n_z|D}.$$

Terms $\langle E^M \rangle$, $\langle H \rangle^J$ describe the electro-magnetic and magneto-electric interaction of the sheets. Terms $\langle E^J \rangle$, $\langle H \rangle^M$ describe electro-electric and magneto-magnetic interaction. All these series can be easily summarized, and we obtain

$$\langle E \rangle = \kappa_{ee}AJ + \kappa_{em}BM \quad (7)$$

and

$$\langle H \rangle = \kappa_{mm}AM + \kappa_{me}BM \quad (8)$$

where it is denoted

$$\kappa_{em} = -\frac{\phi}{2} = \frac{\kappa_{me}}{j\phi}, \quad \kappa_{ee} = \frac{-j\eta}{2} = \frac{\kappa_{mm}}{j\phi\eta^2} \quad (9)$$

and

$$A = \frac{\sin kD}{\cos kD - \cos \beta D}, \quad B = \frac{\sin \beta D}{\cos kD - \cos \beta D} \quad (10)$$

Substituting eqs (7) and (8) into eq (6) we obtain a set

$$(1 - a_{mm}\kappa_{mm}A)M - a_{mm}\kappa_{me}BJ = 0, \quad (11)$$

$$(1 - a_{ee}\kappa_{ee}A)J - a_{ee}\kappa_{em}BM = 0, \quad (12)$$

which immediately leads to the dispersion equation:

$$\left(\frac{1}{a_{mm}} - \kappa_{mm}A \right) \left(\frac{1}{a_{ee}} - \kappa_{ee}A \right) = \kappa_{me}\kappa_{em}B^2 \quad (13)$$

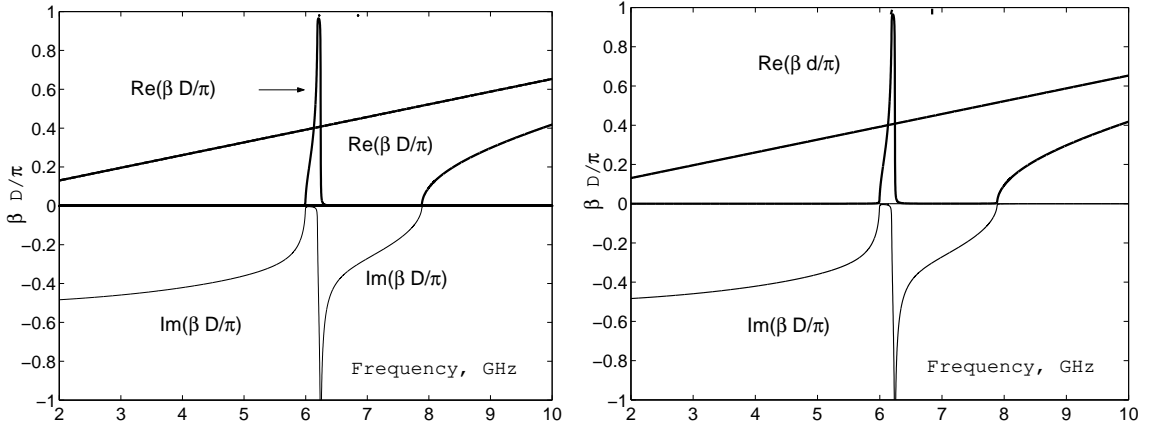


Figure 2: Dispersion curves for our structure without loop loading. Left: perfect wires. Right: copper wires. Straight lines correspond to the trivial solution of the dispersion equation.

Taking into account relations κ , $\hat{a}b$ and $\hat{g}r$ id (which can be written in form $1/a_{ee} = Z_g = j\eta\alpha/2$) one can rewrite \hat{d} isp in a following form:

$$\frac{2}{\phi\eta a_{mm}}(\cos kD - \cos \beta D)\sin kD - (1 + \alpha)\sin^2 kD - \cos^2 \beta D + 1 = 0. \text{ldisp1} \quad (14)$$

This is the needed dispersion equation of our structure. Notice, that for the lossless case, we have obtained the real dispersion equation providing the band structure of our lattice. This equation is valid not only at low frequencies ($kD < 1$), where the grid parameter α is given by $\hat{g}r$ id, it is valid at rather high frequencies where the high-order corrections to α can be taken into account (see e.g. in [20]). Equation \hat{d} isp1 has two solutions. One solution describes the propagation factor of the wave which interacts with the lattice and is polarized so that $E = E_x$, $H = H_y$. Another solution is trivial ($\beta = k$) and corresponds to the case $E = E_y$, $H = H_x$.

The results for the normalized propagation factor versus frequency (in GHz) are shown in Fig. 2. The following parameters of the lattice were picked up: $2d = 2$ mm, $D = 8$ mm, $D_x = 24$ mm, $l = 10$ mm, $Z_0 = 0$ (no loop loading) and $r_0 = 0.02$ mm. The plot at the left of this Figure corresponds to perfectly conducting chains. The plot at the right corresponds to the chains fabricated from copper. The lattice is assumed to be located in the homogeneous dielectric matrix with permittivity $\epsilon_m = 1.5 - j0.001$. The losses of the matrix do not play any visible role, and the dispersion plot at the left is practically the same as for the lossless dielectric.

The resonant band of MRs contains two sub-bands. In the upper half of the resonant band (6.21 – 6.42 GHz) the lossless lattice has the complex mode $\beta D = \pi + j\text{Im}(\beta D)$. This is a well-known mode of metallic photonic crystals. The propagation is suppressed whereas the induced currents are alternating from one chain to another along the z -axis. In the lower half of the resonant band (6.00 – 6.21 GHz) the lossless lattice supports the usual forward wave, and below we will see that this is the domain where $\epsilon_{xx} > 0$ and $\mu_{yy} > 0$. This difference with the known case of SRRs and wires corresponds to the substitution of a series resonance (of SRRs) by a parallel one (of our MRs).

The ohmic losses in MRs visibly shift the resonance. This effect was explained in [12] (for the case when MRs are performed as SRRs) as the result of electromagnetic interaction in the lattice. In the lossy case the complex mode disappears. The lower sub-band still corresponds to the usual (forward-wave) mode propagating with negligible attenuation, whereas the backward wave in the upper sub-band suffers very strong attenuation. Below we will see that this sub-band corresponds to the case $\text{Re}(\epsilon_{xx}) < 0$ and $\text{Re}(\mu_{yy}) > 0$.

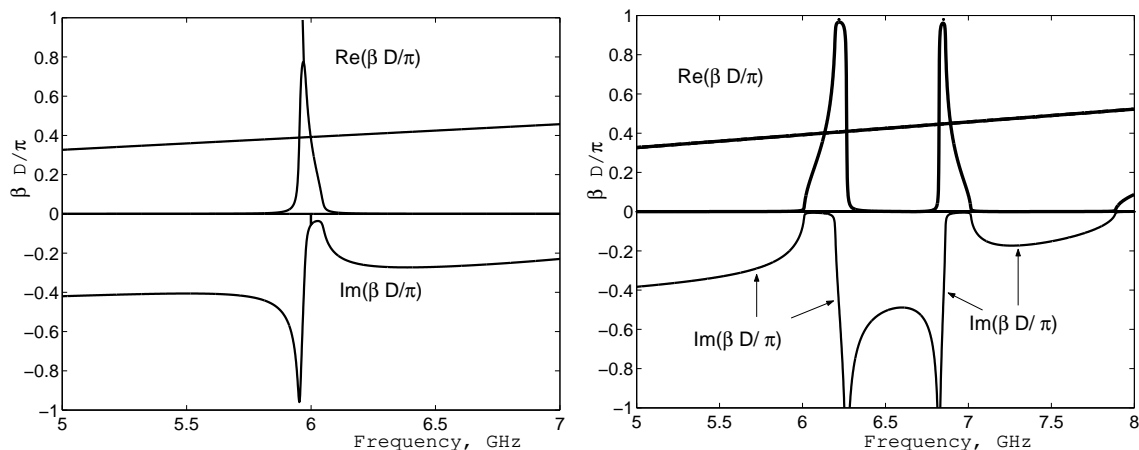


Figure 3: Dispersion curves for two left-handed media from copper wires. Left: the lattice of straight wires and SRRs. Right: our structure with inductive loads. Straight lines correspond to the trivial solutions of dispersion equations.

However one can significantly decrease this attenuation substituting the parallel resonance with the series one. For it we introduce the loading of the loops. The loaded loop can have in the same frequency range both series and parallel resonances. The capacitive loading $Z_0 = 1/j\omega C_0$ gives the series resonance as a first resonance versus frequency. At this resonance our MRs operate as SRRs, and the attenuation of the backward wave turns out to be rather important. No advantages was found for this case in the replacing the SRR by long loops.

The inductive loading $Z_0 = j\omega L_0$ is more useful. It not only shifts the frequencies of the series and parallel resonances of our loop, it also broadens the resonant band. Moreover, the attenuation of the backward wave can be strongly decreased by the appropriate choice of L_0 . In Fig. 3, right part, we show the dispersion plot for the case when $L_0 = 30$ nH (it is a realistic value for a microwave lumped inductance of size 1 mm). Other parameters are the same, but the new length of the loop is chosen $2l = 17$ mm to keep nearly the same frequency range of the resonance. Loaded MRs have now two resonance bands at the frequencies from 0 to 10 GHz. The lower one is still the antiresonance, and the second one is the series resonance. Within both of them there is a sub-band of the backward wave. In the first resonance sub-band the attenuation of this backward wave is very high (this effect will be discussed below). In the second sub-band of the backward wave (near 7 GHz) the attenuation is small (almost invisible in the plot). For comparison the dispersion plot of the two-phase lattice from wires and SRRs is presented in the same Figure (left part). There the attenuation of the backward wave (within 6 – 6.1 GHz) is visible clearly. The period of both wire and SRR lattices was taken the same as for our lattice ($D = 8$ mm), as well as the permittivity of the matrix ($\epsilon_m = 1.5 - j0.001$). The parameters of SRRs were picked up so that to obtain the resonance at nearly the same frequencies: $r_1 = 1.5$ mm (radius of the outer ring), $r_2 = 1.2$ mm (that of the inner ring), wire radius $r_0 = 0.05$ mm. The SRRs also were assumed to be made from copper. The calculations corresponds to the analytical model described in [12]. It is important that the structure suggested in the present paper has smaller attenuation of the backward wave than the lattice of SRRs and straight wires, though the rather large radius $r_0 = 50$ μ m was picked up for the two-phase lattice (versus $r_0 = 20$ μ m picked up for our structure). One can see in the same Figure that the model also predicts for our structure more wide frequency band of the backward wave than for the lattice of SRRs and wires.

3. Material parameters

let us try to consider the structure as a uniaxial magneto-dielectric medium. Then the interacting wave satisfies the following material equations:

$$\mathcal{D}_x = \epsilon_0 \epsilon_m E_x + P_x^{\text{bulk}} = \epsilon_0 \epsilon_{xx} E_x, \quad (15)$$

$$\mathcal{B}_y = \mu_0 H_y + M_y^{\text{bulk}} = \mu_0 \mu_{yy} H_y. \quad (16)$$

Let us find ϵ_{xx} and μ_{yy} . Define the auxiliary parameter γ as

$$\gamma = \eta \frac{P_x^{\text{bulk}}}{M_y^{\text{bulk}}} = \frac{(\epsilon_{xx} - 1) E_x}{\eta (\mu_{yy} - 1) H_y}.$$

From our definitions of J and M it follows that

$$P_x^{\text{bulk}} = \frac{J}{j\phi D_y} = \frac{J}{j\phi D}, \quad M_y^{\text{bulk}} = \frac{M}{D_z} = \frac{M}{D}.$$

From Maxwell's equations together with \mathring{d} and \mathring{b} one has:

$$\frac{E_x}{H_y} = \eta \sqrt{\frac{\mu_{yy}}{\epsilon_{xx}}}$$

Therefore

$$\gamma = \frac{\eta J}{j\phi M} = \frac{(\epsilon_{xx} - 1)}{(\mu_{yy} - 1)} \sqrt{\frac{\mu_{yy}}{\epsilon_{xx}}}. \quad (17)$$

From first or second we easily find J/M . Then final leads to the first equation for material parameters:

$$\frac{(\epsilon_{xx} - 1)}{(\mu_{yy} - 1)} \sqrt{\frac{\mu_{yy}}{\epsilon_{xx}}} = \frac{\eta(1 - a_{mm} \kappa_{mm} A)}{j\phi a_{mm} \kappa_{me}}. \quad (18)$$

For $A(\beta)$ we have the relation $\mathring{a}\mathring{b}$, and β is found from dispersion equation $\mathring{\text{disp}}1$. The second equation is trivial

$$\beta^2 = k^2 \epsilon_{xx} \mu_{yy}. \quad (19)$$

From first and second we find two solutions for ϵ and μ and pick up the true one having the negative imaginary part.

In Fig. 4 we present the real parts of permittivity (solid lines) and permeability (dotted lines). At the left the case of unloaded loops is shown (corresponding to the right part of Fig. 2). At the right the case of loaded loops is presented (corresponding to the right part of Fig. 3). The resonant behavior of permittivity is an illustration of the fact, that a naive understanding of permittivity and permeability of left-handed composites as an arithmetic sum of the permittivity of wire medium and permeability of an artificial magnetic is completely wrong. The electromagnetic interaction of magnetic and electric components of the meta-material tightly relates these two parameters.

One can see that the case without loads (parallel resonance at 6 GHz) corresponds to the case when μ and ϵ are never have negative real parts simultaneously³. The lower sub-band of the parallel resonance band corresponds to the very small attenuation and contains two very narrow frequency bands. In the lower (6 – 6.1 GHz) one the permeability becomes negative,

³Since there is no load the first series resonance of the loop corresponds to 12 GHz. At this resonance the material parameters formally become both negative but lose the physical meaning, since the lattice period 8 mm becomes larger $\lambda/4$.

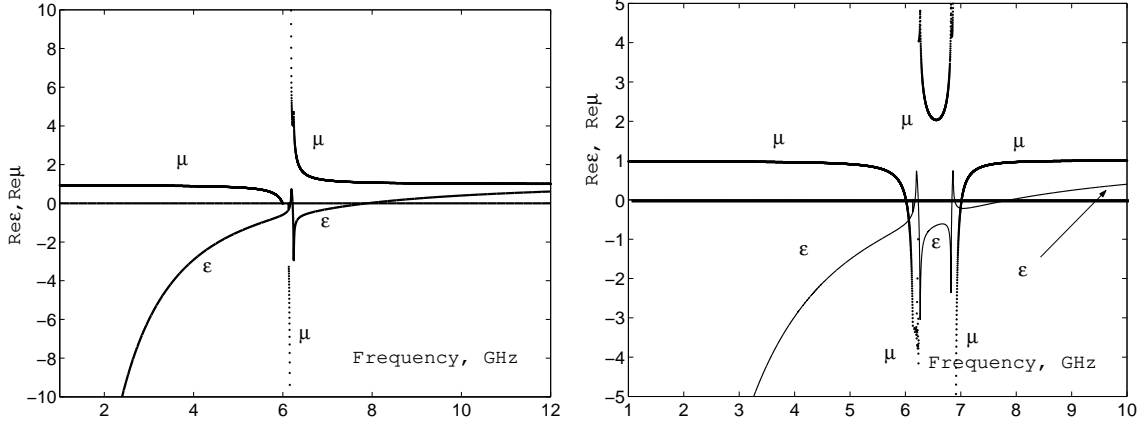


Figure 4: Effective constitutive parameters ϵ_{xx} and μ_{yy} (real parts only) of the lattice from chains of long loops. Left: unloaded loops. Right: loaded loops.

but the permittivity simultaneously becomes positive. This is still the stop-band in Fig. 2 (the right part of this Figure corresponds to the copper wires). In the upper one (6.1 – 6.2 GHz) the permeability becomes positive, whereas the resonant permittivity is still positive. This is the band of the forward wave shown in Fig. 2. The frequencies 6.2 – 6.24 GHz are the upper sub-band of the resonant band in which there appears a strong attenuation, the imaginary parts of material parameters become very large with respect to the real parts, and $\text{Re}(\epsilon_{xx}) < 0$, whereas $\text{Re}(\mu_{yy}) > 0$. This is the band of the attenuating backward wave shown in Fig. 2, right part (in the lossless case, presented in Fig. 2 at the left, it is not a backward wave but a complex mode).

Backward wave shown in the right parts of Figs. 2 and 3 which (in the lossy case) replaces the complex mode of a lossless lattice and which corresponds to the parallel resonance of MRs has nothing to do with left-handed medium. When the imaginary parts of material parameters are larger than their real parts the group velocity has no physical meaning and the negative refraction cannot be observed for real signals. Moreover, this is not a continuous medium at all. Huge values of $\text{Im}(\mu_{yy})$ mean that the characteristic scale of the field variation is smaller than the period, and the material parameters we calculated for this sub-band have no physical meaning. So, magnetic scatterers with parallel resonance are useless for obtaining the left-handed medium. This makes unloaded long loops be not prospective for this purpose.

However, the case of loaded loops looks like very promising. In Fig. 5 the dispersion curves shown in the right part of Fig. 3 is reproduced. It is plotted within the second resonant band of our MRs so that to see the resonant dispersion in details. In the right part of the Figure one shows in details the resonant behavior of effective constitutive parameters. One can see that the lower sub-band of the series resonance band (6.82 – 6.87 GHz) corresponds to the forward wave propagating with very strong attenuation. This wave substitutes the complex mode of lossless lattice, and within this sub-band one has $\text{Re}(\mu_{yy}) > 0$ whereas $\text{Re}(\epsilon_{xx}) < 0$ (see also Fig. 4, right part). Within the upper sub-band of the series resonance (from 6.87 to 7.01 GHz) one has the backward wave regime. Within this band the imaginary parts of material parameters do not exceed 4% of their real parts. The band 6.93 – 7.01 GHz corresponds to values of the product $|\sqrt{\epsilon_{xx}\mu_{yy}}|$ of the order unity (which is promising for application of the layer from such a meta-material as a lens). Imaginary parts of material parameters are very small within this band (1 – 2%).

At the first glance, one can think that the inductive loading of long loops does not change their frequency properties. Unloaded loops as well as loaded ones exhibit a set of parallel and series resonances versus frequency. For $l = 10$ mm we have the first parallel resonance at 6 GHz

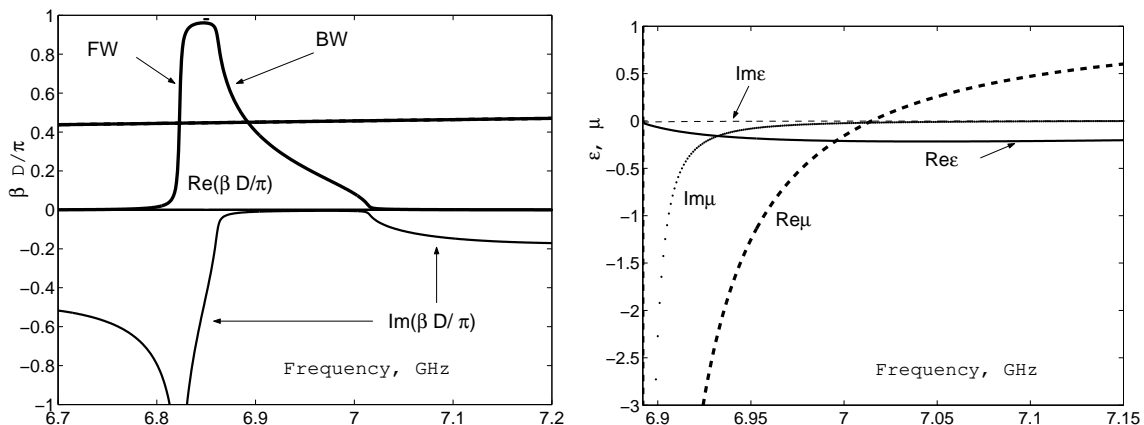


Figure 5: Left: dispersion plot within the resonant band of loaded loops from copper wires. Forward wave (FW) is within the lower-sub-band. Backward wave (BW) is within the upper sub-band. Right: effective constitutive parameters ϵ_{xx} and μ_{yy} (real and imaginary parts) within the band of the backward wave.

(see Fig. 2), the first series resonance of unloaded loop holds at 12 GHz, the second parallel resonance at 16 GHz, etc. To obtain a series resonance at 6 GHz with unloaded loops it is enough to take a loop with $l = 20$ mm. However, the calculations show that at this resonance the structure with unloaded loops exhibits the very narrow frequency band of the backward wave (23 MHz versus 124 MHz obtained above for loaded loops) and the magnetic losses for unloaded loops are also higher than we obtained above for the case of inductive loading of loops with $2l = 17$ mm. The loading makes the frequency positions of parallel and series resonances not equidistant, broadens the resonant band and decreases the losses in the left-handed regime.

4. Conclusion

We have suggested a new variant of a uniaxial left-handed material for microwave applications which theoretically exhibits very small losses in a comparatively wide frequency band (2%). The comparison with the two-phase lattice of straight wires and split-ring resonators exhibits the better characteristics of the proposed structure. This is the result of substituting the simple circuit resonance of capacitively loaded small magnetic resonators (SRRs) by the resonance of a loaded transmission line. Our magnetic resonators are long and narrow inductively loaded loops. In the present paper we suggest only an approximate analytical model, which is, however, self-consistent and satisfying the basic physical conditions. The further numerical simulations are necessary. The material can be realized using the planar technology which makes possible its experimental testing in the next future.

References

- [1] V.G. Veselago, "The electrodynamics of substances with simultaneously negative values of ϵ and μ ", *Soviet Physics Uspekhi*, vol. 10, pp. 509-514, 1968. (originally in Russian in *Uspekhi Fizicheskikh Nauk*, vol. 92, no. 3, pp. 517-526, July 1967)
- [2] J.B. Pendry, "Negative refraction makes a perfect lens", *Phys. Rev. Lett.*, vol. 85, no. 18, pp. 3966-3969, 2000.
- [3] R.A. Shelby, D.R. Smith and S. Schultz, "Experimental verification of a negative index of refraction", *Science*, vol. 292, pp. 77-79, 2001.
- [4] K. Lu, J. McLean, R. Gregor, C. Parazzoli and M.H. Tanielian, "Free space focused beam characterization of left-handed materials", *Appl. Phys. Lett.*, vol. 82, pp. 2535-2537, 2003.

- [5] A. Houck, J. Brack, I. Chuang, “Experimental observation of a left-handed material that obeys Snell’s law”, *Phys. Rev. Lett.*, vol. 90, pp. 137401(1-4), 2003.
- [6] J.B. Pendry, A.J. Holden, D.J. Robbins, and W.J. Stewart, “Magnetism from conductors and enhanced nonlinear phenomena”, *IEEE Trans. Microw. Theory Tech.*, vol. 47, no. 11, pp. 2075-2084, 1999.
- [7] R. Marques, F. Medina and R. Rafii-Idrissi, “Role of bi-anisotropy in negative permeability and left-handed metamaterials”, *Phys. Rev. B*, vol. 65, pp. 144440(1-4), 2002.
- [8] N. Garcia and M. Nieto-Vesperinas, “Negative refraction does not make perfect lens”, *Phys. Rev. Lett.*, vol. 88, no. 12, pp. 122501(1-3), 2002.
- [9] E.V. Ponizovskaya, M. Nieto-Vesperinas and N. Garcia, “Losses for microwave transmission meta-materials for producing left-handed materials. The strip wires”, submitted to *Phys. Rev. B*, available at *cond-mat/0206429*.
- [10] A.L. Pokrovsky and A.L. Efros, “Electrodynamics of metallic photonic crystals and the problem of left-handed materials”, *Phys. Rev. Lett.*, vol. 89, no. 10, pp. 093901(1-4), 2002.
- [11] P. Marokos and C.M. Soukoulis, “Transmission studies of the left-handed materials”, *Phys. Rev. B*, vol. 65, pp. 033401, 2002.
- [12] C.R. Simovski and B. Sauviac, “Role of wave interaction of wires and split-ring resonators for the losses in a left-handed composite”, submitted to *Phys. Rev. E*, accessible at *arxiv.org*.
- [13] C.R. Simovski and S. He, “Frequency range and explicit expressions for negative permittivity and permeability for an isotropic medium formed by a lattice of perfectly conducting Omega-particles”, *Phys. Lett. A*, vol. 311, pp. 254-263, 2003.
- [14] R.W. Ziolkovski, “Design, fabrication and testing of double negative metamaterials”, *IEEE Trans. Antennas. Propag.*, vol. 51, no. 7, pp. 1516-1529, 2003.
- [15] S.A. Tretyakov, I.S. Nefedov, C.R. Simovski and S.I. Maslovski, “Modelling and microwave properties of artificial materials with negative parameters”, in *Advances in electromagnetics of complex media and meta-materials*, S. Zouhdi, A. Sihvola and M. Arsalane (eds), NATO Series II, vol. 89, Kluwer Academic Publishers, pp. 99-122, 2002.
- [16] F. Gardiol, *Electromagnétisme*, Dunod Université, 1987 (in French).
- [17] S.A. Tretyakov and A.J. Viitanen, Plane waves in regular arrays of dipole scatterers and effective medium modelling, *JOSA*, vol. 17, No 10, pp. 1791-1797, 2000.
- [18] C.R. Simovski, *Weak spatial dispersion in composite media*, Polytechnika Publishers, St. Petersburg, 2003 (in Russian).
- [19] B. Sauviac, E. Verney, C. Simovski and G. Rouffié, Fabrication d’un matériaux main gauche artificiel, *Journée de Caractérisation Matériaux Microondes*, La Rochelle, France, March 31, 2004.
- [20] S.A. Tretyakov, *Analytical modelling in applied electromagnetics*, Artech house, Boston-London, 2002.
- [21] C.R. Simovski, P. Belov and S. He, “Backward wave region and negative material parameters of a structure formed by lattices of wires and split-ring resonators”, *IEEE Trans. Antennas. Propag.*, vol. 51, no. 10, pp. 2582-2591, 2003.